

Deciphering the Remnants of Core-Collapse Supernovae: Reconstructing Progenitor Star Properties and Explosion Mechanisms

Salvatore Orlando^{a,*}

^aINAF - Osservatorio Astronomico di Palermo, Piazza del Parlamento 1, 90134 Palermo, Italy

E-mail: salvatore.orlando@inaf.it

Recent observations of the supernova remnant (SNR) Cassiopeia A (Cas A) with the James Webb Space Telescope (JWST) have revealed unprecedented details of its structure, including an intricate network of ejecta filaments and an enigmatic structure known as the "Green Monster" (GM), characterized by a pockmarked appearance with nearly circular holes and rings. These discoveries offer unique insights into the mechanisms governing supernova (SN) explosions and the subsequent evolution of ejecta and circumstellar medium (CSM) interactions.

In this contribution, I present recent theoretical work based on high-resolution three-dimensional (3D) hydrodynamic (HD) and magnetohydrodynamic (MHD) simulations of a neutrino-driven SN explosion resembling Cas A. The models follow the system from core collapse to an age of ~ 1000 years, with the aim of investigating the origin and evolution of these newly observed structures. The simulations incorporate key physical processes, including neutrino-driven explosion dynamics, hydrodynamic instabilities, Ni-bubble effects, and radiative losses, while accounting for deviations from ionization equilibrium and electron–proton temperature equilibration.

The new studies show that a web-like network of ejecta filaments, closely resembling those observed by JWST, naturally forms during the early stages of the explosion as a consequence of hydrodynamic instabilities and the dynamic interplay of hot neutrino-driven bubbles. These filaments preserve a "memory" of the initial explosion conditions before being gradually disrupted by the reverse shock over centuries. In parallel, the peculiar morphology of the GM can be reproduced by the interaction of dense clumps and fingers of ejecta with an asymmetric, forward-shocked CSM shell. Radiative cooling and non-equilibrium ionization further enhance fragmentation, producing dense knots and thin filaments that penetrate the shell and create the observed network of holes and rings.

Our model highlights how the complex structures observed today in Cas A reflect both the imprint of the early SN explosion and the later interactions of ejecta with the surrounding medium, offering a unified view of the remnant's rich morphology.

Multifrequency Behaviour of High Energy Cosmic Sources - XV (MULTIF2025)
9-14 June, 2025
Mondello, Palermo, Italy

*Speaker

1. Introduction

Supernova remnants (SNRs), the outcomes of supernova (SN) explosions, can be essential laboratories for probing both the physics of core-collapse SNe and the late evolutionary stages of massive stars. When a massive star collapses, the explosion mechanism generates a rich interplay of hydrodynamic instabilities, asymmetric plumes, and turbulent mixing between nucleosynthetic layers [1–3, 13, 14, 47, 49]. These processes, occurring within the first few seconds after core collapse, are usually inaccessible to direct observation. Yet, as the stellar debris expands and interacts with the circumstellar and interstellar environment, a SNR preserves these signatures in its structure, composition, and dynamics [29, 32, 33, 36]. The geometry of the ejecta, the distribution of heavy elements, and the morphology of shocked and unshocked material all carry the imprint of the explosion engine. Studying young SNRs therefore allows us to reconstruct aspects of the explosion mechanism that cannot be directly inferred from SN light curves or spectra.

At the same time, the outer morphology of a SNR, particularly the shape and behavior of the forward and reverse shocks, also retains information about the environment through which the remnant expands [20, 21, 37, 38, 46]. In the case of young remnants, this environment is the circumstellar medium (CSM), which reflects the mass-loss history of the progenitor star [25, 31, 35]. Massive stars undergo complex evolutionary phases involving winds, eruptions, and episodes of enhanced mass loss. These processes create circumstellar shells, bubbles, and density gradients that strongly influence the remnant's evolution once the SN blast wave reaches them. As a result, young SNRs encapsulate both the physics of the SN explosion and the final centuries or millennia of the progenitor's life, bridging stellar evolution and SN physics.

Among all Galactic remnants, Cassiopeia A (Cas A) stands as the most informative example of this dual role. With an age of only ≈ 350 years [6, 44], Cas A is one of the few SNRs young enough that many fine-scale structures originating from the explosion are still visible. Its proximity (≈ 3.4 kpc, [39]) allows high-resolution observations across the electromagnetic spectrum, revealing a wealth of morphological features [5, 10–12, 16, 22, 23, 42, 45]: Fe-rich plumes that extend beyond lighter elements, an inversion of nucleosynthetic layers, rapidly moving knots and jets, and strong asymmetries in both shocked and unshocked material. These characteristics have made Cas A the benchmark case for testing multidimensional SN models and for constraining the nature of mixing instabilities, neutrino-driven convection, and asymmetries in the explosion engine.

The advent of JWST has profoundly enhanced this picture. Infrared imaging of Cas A has unveiled a complex network of unshocked, O-rich filaments in its interior [24, 40], exhibiting sub-parsec structures with extraordinary sharpness. Additionally, JWST observations of the near (blueshifted) side of the remnant have revealed the striking "Green Monster" [4] (GM): a region filled with circular holes, partial rings, and arc-like cavities in shocked circumstellar material. These discoveries pose new challenges: the internal filaments require an explanation rooted in the earliest instabilities of the explosion, while the GM demands a mechanism involving the interaction between ejecta clumps and the progenitor's circumstellar environment.

Two recent numerical works, one dedicated to the origin of the filamentary interior network [27], and the other to the formation of the GM's holes and rings [26], address these challenges with fully three-dimensional (3D) simulations following Cas A's evolution from the core-collapse to the present day and, extending the evolution to the age of 1000 years [36]. Together, these studies aim

to link the imprints of the explosion engine, the behavior of the ejecta, and the structure of the CSM into a coherent narrative. The present review summarizes the main results.

2. Modeling Strategy

The two studies build upon a unified numerical framework designed to follow the evolution of Cas A continuously from the first instants after core collapse to the present remnant stage (see Orlando et al. [36] for the details of the simulations). The modeling begins with a 3D neutrino-driven explosion simulation, specifically the W15-2-cw-IIb model [48], which provides the structure of the ejecta only hours after the launch of the outgoing shock. This model is based on a $15 M_{\odot}$ zero-age main sequence progenitor that was artificially stripped of most of its hydrogen envelope to reproduce a Type IIb configuration appropriate for Cas A, resulting in a compact pre-supernova star with a final radius of $\sim 21.5 R_{\odot}$. The explosion was calibrated to reach a final kinetic energy of $\sim 1.5 \times 10^{51}$ erg with a total mass of ejecta of $3.3 M_{\odot}$, and to synthesize approximately $\sim 0.1 M_{\odot}$ of radioactive ^{56}Ni . Only about $0.3 M_{\odot}$ of hydrogen-rich material was retained in the progenitor structure, implying that roughly $8 - 10 M_{\odot}$ of stellar mass was lost during the late evolutionary stages and injected into the surrounding CSM. At this early time, the explosion already contains the key physical ingredients that govern the later morphology of the remnant: large-scale neutrino-heated bubbles, strong Rayleigh-Taylor (RT) instabilities, and high-velocity Ni-rich plumes punching through the star's composition layers. These features break spherical symmetry from the outset and establish a network of density contrasts, plumes, and cavities that later evolve into the filaments and clumps observed in the remnant.

This initial configuration is mapped to a large computational grid and evolved for centuries using high-resolution 3D hydrodynamics or magnetohydrodynamics (MHD) when appropriate. The simulations track the free expansion of the ejecta, the formation of the reverse shock, and the progressive interaction with the surrounding CSM. They incorporate a comprehensive set of physical processes essential to capturing the behavior of a young SNR: optically thin radiative cooling, which allows dense ejecta knots to condense and survive; non-equilibrium ionization, which governs the thermal state of both shocked and unshocked gas; and heating from radioactive decay, in particular the expansion of Ni-rich bubbles that compress O-rich layers. Chemical elements are followed with passive tracers, enabling the reconstruction of spatial distributions for individual species such as O, Si, Fe, and Ti. Thanks to a remapping technique (e.g., Orlando et al. [30, 33]) and high spatial resolution (2048^3 cells), the simulations resolve structures down to ~ 0.01 pc at the age of Cas A, comparable to the spatial resolution of JWST.

To investigate the GM, the evolving ejecta interact with a thin, dense circumstellar shell positioned at roughly 1.5 pc from the explosion center. This shell, previously proposed to explain Cas A's reverse-shock asymmetry [35], is modeled as a narrow, high-density layer, likely produced by a major mass-loss episode of the progenitor star shortly ($10^4 - 10^5$ years) before core collapse. Its structure is asymmetric, with enhanced density on the blueshifted side of the remnant (the region where the GM is observed). This shell plays a crucial role in shaping the late-time morphology, acting as a barrier that is struck and perforated by the fastest ejecta clumps.

Finally, the simulations are rotated into the orientation that best matches the observed distribution of Fe- and Ti-rich ejecta in Cas A. Synthetic projections of density, temperature, and

element-specific emission allow a direct comparison with JWST, Chandra, and NuSTAR observations. Through this combination of realistic explosion physics, detailed microphysics, and careful observational alignment, the models provide a physically grounded, high-fidelity reconstruction of Cas A's evolution from core collapse to its present, highly structured remnant state.

3. Results

To understand the new structures revealed in Cas A by JWST, the simulations examine different but complementary aspects of the remnant's evolution. Sect. 3.1 focuses on the internal, unshocked O-rich filamentary network, tracing its origin back to the earliest seconds of the explosion, while Sect. 3.2 investigates the GM, showing how its system of holes and rings arises from the interaction between ejecta clumps and a dense circumstellar shell. Together, these works [26, 27] provide a coherent physical interpretation linking the explosion mechanism, the evolution of the ejecta, and the imprint of the progenitor's mass-loss history.

3.1 Origin of the Filamentary O-Rich Network

The simulations demonstrate that the intricate web of unshocked, O-rich filaments revealed by JWST in the interior of Cas A is not a product of late-time hydrodynamic evolution in the SNR, but instead a direct fossil imprint of the explosion mechanism itself, established within the first second after core collapse [27]. In the model, the neutrino-driven engine produces large, rising plumes of neutrino-heated material that immediately break spherical symmetry. As the shock moves outward through the stratified stellar layers, these plumes drive vigorous mixing across nucleosynthetic boundaries.

In the first minutes to hours after shock launch, the formation and growth of hot, buoyant, Ni-rich bubbles further amplify the initial asymmetries. Their expansion pushes and compresses the surrounding layers enriched in oxygen, carbon, neon, and magnesium, carving them into elongated sheets. At the same time, RT instabilities rapidly stretch, corrugate, and fragment these dense structures, producing a complex filamentary pattern at the time when the shock reaches the stellar surface (see Fig. 1).

In the following months, radioactive decay of Ni to Co and later to Fe releases additional energy that inflates the originally Ni-rich ejecta, an effect known as the Ni-bubble phenomenon. This continued expansion reinforces the compression of the surrounding intermediate-mass layers, sharpening the internal structure and further refining the filamentary network. As a result, by the time the remnant is only a few years old, the simulations already display a highly organized, interconnected web of dense, O-rich filaments occupying the remnant's unshocked interior.

At the current age of ~ 350 years, the filamentary network in the models exhibits an analogous geometry, hierarchy, and characteristic thickness (~ 0.01 pc) as JWST images (see Fig. 2): a tangled internal "spider-web" of O-rich structures occupying the interior of the remnant, bounded by the cavities created by fast-rising Fe-rich plumes. Heavier material such as Fe and Ti remains largely concentrated within these plumes and cavities and does not participate in the extended filamentary web. The spatial anticorrelation between shocked Fe-rich structures and O-rich filaments thus emerges naturally from the explosion physics, without requiring fine-tuned assumptions in the remnant phase (see Orlando et al. [27] for the details).

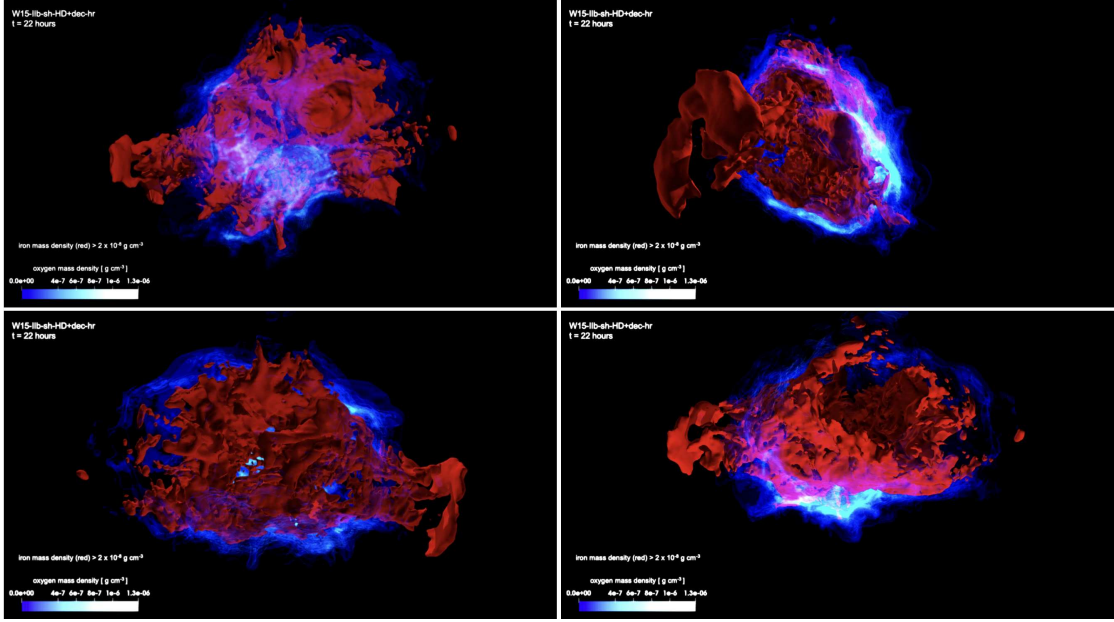


Figure 1: Distribution of unshocked Ni-rich ejecta (red isosurface; $\rho_{\text{Ni}} > 2 \times 10^{-8} \text{ g cm}^{-3}$) a few hours after shock breakout (≈ 22 hr after core collapse) for model W15-IIb-sh-HD+dec-hr. Unshocked O-rich ejecta are shown via volume rendering (blue palette). The upper left panel shows the front view as seen from Earth. The remaining panels show perspectives from arbitrary orientations. An interactive 3D visualization of the O and Ni distributions is available at <https://skfb.ly/psXKs>.

The simulations also roughly reproduce the observed distribution of unshocked mass: at Cas A’s present epoch, roughly one solar mass of ejecta remains unprocessed by the reverse shock, consistent with observational estimates. The unshocked component is dominated by oxygen, with smaller contributions from helium, carbon, neon, magnesium, and silicon, and only trace amounts of Fe-group nuclei. These masses and abundances fall within observational constraints from infrared and X-ray studies.

Once the reverse shock encounters the filamentary ejecta, beginning a few decades after explosion, the network starts to degrade. RT and Kelvin–Helmholtz instabilities generated by the shock interaction gradually erode the fine-scale structure, fragmenting the filaments and dispersing their material into the shocked interior. The modeling predicts that although the network is still prominently visible today, it is transient: as Cas A approaches ~ 700 years of age, the filaments lose coherence and the JWST-scale morphology will no longer be recognizable. We note that this also implies that similar filament networks in older Galactic remnants would have been erased, making Cas A a uniquely timed system for observing the explosion’s hydrodynamic fingerprint.

Finally, the study emphasizes that the formation of the filamentary network depends predominantly on the physics of the SN explosion, not on the properties of the CSM or later remnant evolution. Even in simulations lacking strong circumstellar shaping, the network forms, evolves, and reaches a structure in remarkable agreement with observations. Thus, JWST’s newly revealed filaments provide the clearest evidence to date that young SNRs can function as direct archaeolog-

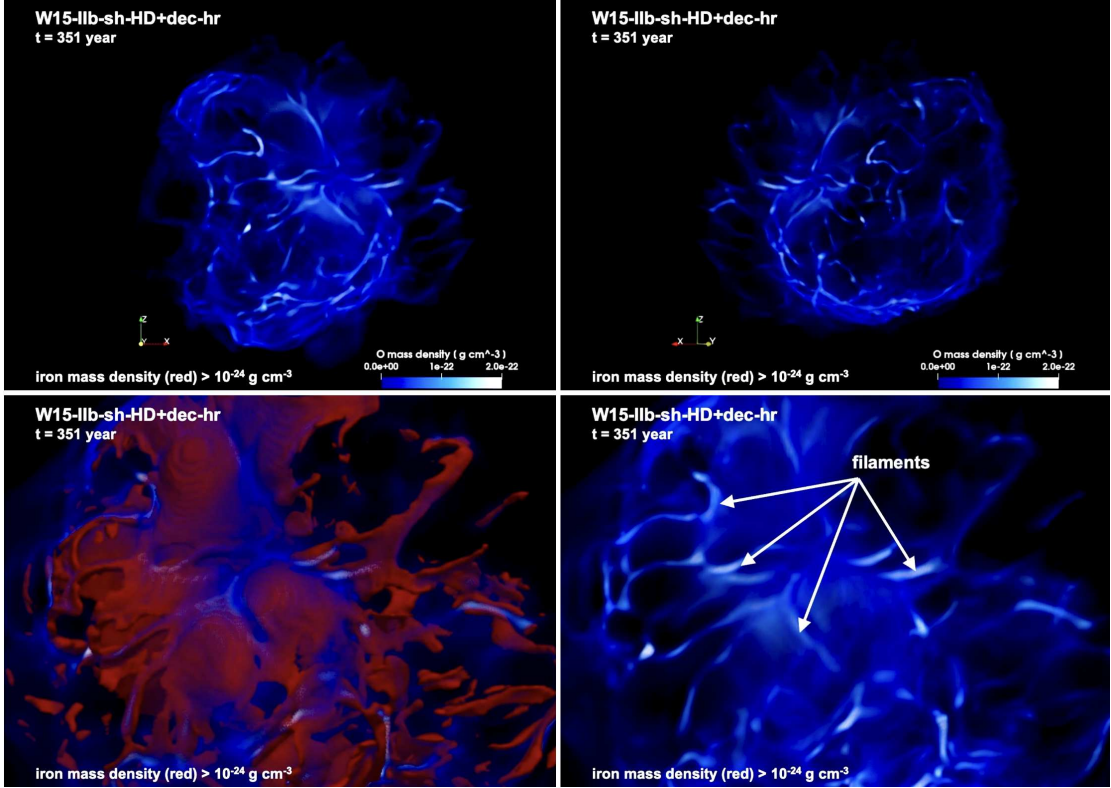


Figure 2: Upper panels: Distribution of unshocked O-rich ejecta visualized via volume rendering (blue palette) at the age of Cas A for model W15-IIb-sh-HD+dec-hr. The color scale is shown in the bottom-right corner of each panel. Rendering opacity is proportional to the plasma density, highlighting the denser structures. The upper-left panel shows the front view as seen from Earth, while the upper-right panel shows a side view from a vantage point to the west (positive x -axis). Lower panels: Zoom into the central region revealing filamentary O-rich ejecta. In the lower-left panel, the O-rich distribution (blue) is shown together with the unshocked Fe-rich ejecta, displayed as a red isosurface corresponding to Fe densities above $10^{-24} \text{ g cm}^{-3}$. An interactive 3D visualization of the O and Fe spatial distributions at the age of Cas A is available at <https://skfb.ly/psXKr>.

ical records of the earliest instabilities of the explosion engine, allowing modern simulations and observations to probe the inner seconds of a core-collapse event centuries after it occurred.

3.2 Origin of the Green Monster

The simulations also show that the GM (the large, pockmarked, ring-filled region identified by JWST on the blueshifted, near side of Cas A) arises naturally from the interaction of fast, clumpy SN ejecta with a thin, dense circumstellar shell produced by the progenitor star before explosion [26]. In the simulations, this shell lies at a radius of about 1.5 pc, with a thickness of only ~ 0.02 pc and enhanced density in the northwest direction (see Orlando et al. [35] for more details), matching roughly the observed location of the GM. When the ejecta, shaped by early mixing instabilities in the SN, expand into this structure, dense radiatively cooled RT fingers of ejecta collide with the shell at several thousand kilometers per second, leading to highly characteristic morphological

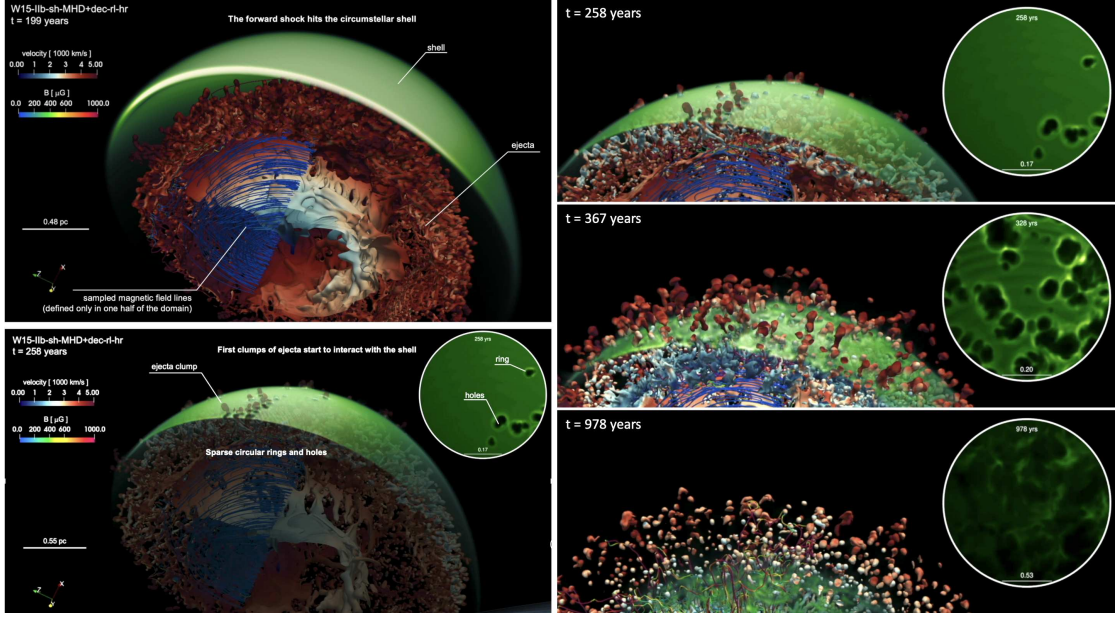


Figure 3: 3D visualization of the ejecta-shell interaction in the Cas A SNR from model W15-IIb-sh-MHD+dec-r1-hr. The irregular isosurface represents ejecta with mass density exceeding $10^{-23} \text{ g cm}^{-3}$, with colors indicating the radial velocity in units of 1000 km s^{-1} (color scale shown in the left panels). The green volume rendering depicts the mass density of the shocked shell material. The sequence spans the evolution from the moment the forward shock first encounters the shell at $t \approx 200$ years (upper-left panel) to the later remnant stage at $t \approx 1000$ years (lower-right panel). The panels on the right show the remnant-shell interaction at three representative epochs, with times indicated in the upper-left corner of each panel. The upper-right inset provides a detailed view of the shell structure, showing the progressive development of holes and ring-like features produced by the interaction with the ejecta. For clarity, magnetic field lines (color scale shown in the left panels) are shown only within a selected sub-volume, highlighting the complexity of the magnetic configuration while preserving a clear view of the ejecta structure in other regions of the remnant. Interactive 3D visualizations of the remnant-shell interaction are available at <https://skfb.ly/psYpK> and <https://skfb.ly/pt7wt>.

signatures that directly correspond to the JWST data. Figure 3 shows the different phases during the interaction of the remnant with the shell and the formation of the holes and rings.

In the simulations, the dense RT fingers produced by the explosion behave effectively as ballistic streams as they encounter the circumstellar shell. Their high velocity allows them to punch through the shell, opening narrow perforations in its structure. The material displaced by the impact is swept laterally and accumulates around the penetration site, forming near-circular rims that outline the resulting holes. Figure 4 illustrates the details of this interaction for a small portion of the remnant shell interaction. When several RT fingers strike the shell in close proximity, their effects overlap, producing compound, irregular, or partially merged rings that reproduce the complex "Swiss-cheese" appearance characteristic of the GM region observed by JWST.

Radiative cooling plays a decisive role, allowing the fingers to reach extremely high density contrasts relative to the shell and remain thin and coherent long enough to create clean perforations

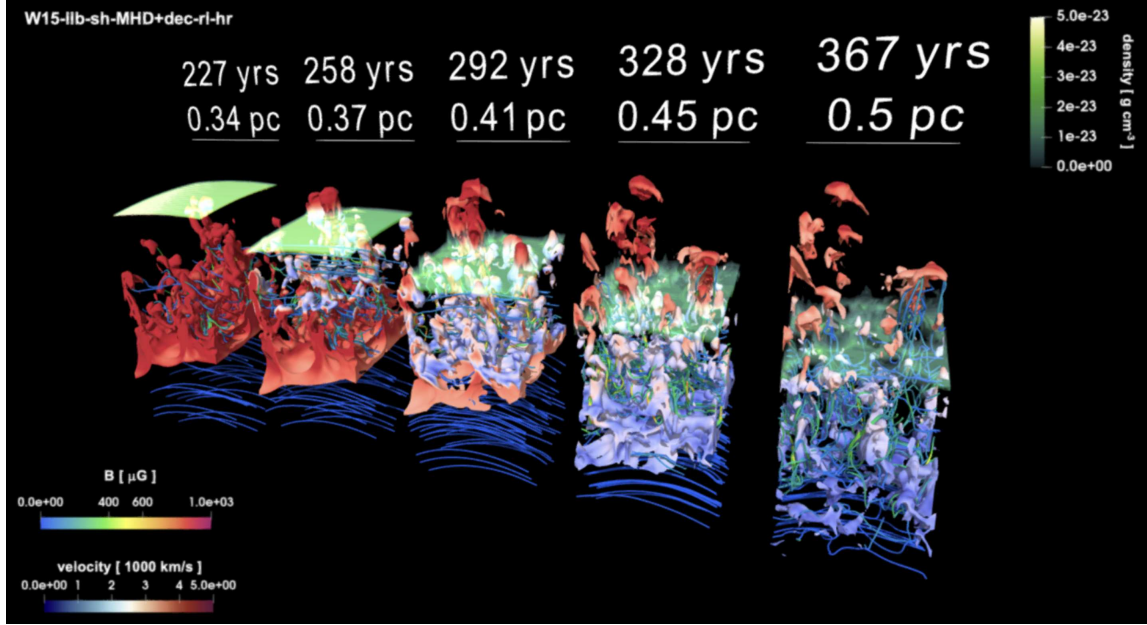


Figure 4: Formation of holes and ring-like structures during the interaction between the ejecta and the shocked shell in model W15-IIb-sh-MHD+dec-r1-hr. The irregular isosurface traces the ejecta, while the green volume rendering shows the mass density of the shocked shell material, as illustrated in Fig. 3. The sequence follows the evolution from the moment the ejecta fingers first encounter the shell at $t \approx 227$ years (left) to a more advanced remnant stage at $t \approx 367$ years (right), corresponding to the age of Cas A. An interactive 3D visualization of the ejecta fingers protruding through the shell is available at <https://skfb.ly/ptFHY>.

with a size comparable to that observed rather than dispersing upon impact. In models that include magnetic fields, the knots are confined even more efficiently, strengthening their ability to survive and burrow through the shell. The simulations also show that the appearance of the GM is dominated not by optical depth or viewing-angle effects but by real physical cavities created in the shocked circumstellar material.

The sizes of the simulated holes (typically around 5 arcseconds, with a distribution extending from ~ 1 to > 10 arcseconds) match well with JWST measurements. A minority of synthetic holes are larger than observed and could be due to the circumstellar shell being located slightly farther from the explosion center in the actual system or possessing a more complex structure than represented in the models. The chemical composition inside the holes is heavily enriched in O-, C-, and Ne-rich material, reflecting the intermediate-mass layers of the progenitor star and providing clear predictions for future spectroscopic confirmation.

4. Conclusions

The recent simulations describing Cas A demonstrate the power of following the evolution of a core-collapse explosion in a fully self-consistent manner: from the progenitor star through the SN event and into the SNR phase. The studies discussed here show that many of the most

striking morphological features revealed by JWST in Cas A cannot be understood if the SNR is modeled without connecting the different phases of evolution, from the progenitor star to the SNR. Instead, they arise naturally from physical processes occurring much earlier: minutes, hours, or even seconds after core collapse for the filaments shaping the remnant's interior, and centuries to millennia before the SN event in the case of the GM. The filamentary O-rich network is a fossilized record of the neutrino-driven instabilities and mixing processes that shaped the explosion engine, while the GM owes its origin to the interaction of the resulting ejecta structures with a circumstellar shell created by the late stages of the progenitor's evolution. These features therefore encapsulate, within a single remnant, the history of both the explosion mechanism and the mass-loss behavior of the star that produced it.

These studies highlight the need for models that seamlessly bridge stellar evolution, SN dynamics, and long-term remnant development. For decades, theoretical studies have tended to treat these phases separately, largely because of the complexity of simulating such a wide range of time and spatial scales. However, the unprecedented sensitivity and angular resolution of instruments such as JWST and future facilities now reveal structures that directly connect these phases in observable detail. Under these circumstances, it becomes essential to model the entire evolutionary chain in a unified framework capable of tracking how instabilities seeded in the explosion produce observable signatures centuries later, and how the circumstellar environment imprinted by the progenitor star shapes the propagation and appearance of the ejecta.

Self-consistent models of this kind do not merely reproduce images; they allow young SNRs to function as archaeological records of the explosion engine, preserving the fingerprints of neutrino heating, hydrodynamic instabilities, and radioactive energy deposition. At the same time, they probe the final centuries of stellar evolution, revealing the density, geometry, and asymmetries of late stellar winds and eruptive mass loss. Cas A is currently the most powerful demonstration of this approach, but as new observatories continue to discover and resolve young remnants across our Galaxy and the Local Group, similar studies will become increasingly important. Another remarkable example is SN 1987A, whose ongoing interaction with its inhomogeneous CSM provides an unparalleled laboratory for testing explosion models, progenitor mass-loss histories, and the transition from SN to SNR. Recent observations are now revealing previously inaccessible details of the ejecta structure in SN 1987A [7, 15, 17–19, 21, 43], providing the crucial spatial, chemical, and dynamical information needed to identify the underlying explosion mechanism and to constrain the nature of the progenitor star [8, 9, 29, 33, 41, 50].

In this context, the synergy between high-fidelity simulations and high-quality multiwavelength observations marks a new era in the study of massive stars and core-collapse SNe. By linking the physics of the progenitor, the explosion, and the remnant in a single, continuous evolutionary narrative, we can now extract physical information that was previously inaccessible, constraining the operation of the SN engine, the role of neutrino-driven turbulence, the development of mixing and RT instabilities, and the nature of massive star mass loss immediately before collapse. This approach promises to transform young remnants like Cas A (and SN 1987A) into precise diagnostic tools, enabling us to move beyond phenomenology and toward a deeper physical understanding of how massive stars end their lives.

Acknowledgments

We thank an anonymous referee for their suggestions that improved our paper. Many colleagues have contributed to the findings reported here; in particular, I am grateful to H.-T. Janka and A. Wongwathanarat for providing the supernova explosion model, and to D. Milisavljevic for leading the analysis of the JWST observations. Additional key contributions were provided by (in alphabetical order) F. Bocchino, I. De Looze, D. Dickinson, E. Greco, M. Miceli, S. Nagataki, M. Ono, D. Patnaude, J. Rho, V. Sapienza, and T. Temim, whose efforts were fundamental to the success of the project. I acknowledge partial financial contribution from the PRIN 2022 (20224MNC5A) - “Life, death and after-death of massive stars” funded by European Union – Next Generation EU and from the INAF Theory Grant “Supernova remnants as probes for the structure and mass-loss history of the progenitor systems”. The navigable 3D graphics have been developed in the framework of the project 3DMAP-VR (3-Dimensional Modeling of Astrophysical Phenomena in Virtual Reality; [28, 34]) at INAF-Osservatorio Astronomico di Palermo.

References

- [1] Blondin, J. M., Mezzacappa, A., & DeMarino, C. 2003, *ApJ*, 584, 971
- [2] Burrows, A. & Vartanyan, D. 2021, *Nature*, 589, 29
- [3] Burrows, A., Vartanyan, D., Dolence, J. C., Skinner, M. A., & Radice, D. 2018, *Space Science Reviews*, 214, 33
- [4] De Looze, I., Milisavljevic, D., Temim, T., et al. 2024, *ApJ*, 976, L4
- [5] DeLaney, T., Rudnick, L., Stage, M. D., et al. 2010, *ApJ*, 725, 2038
- [6] Fesen, R. A., Hammell, M. C., Morse, J., et al. 2006, *ApJ*, 645, 283
- [7] Fransson, C., Barlow, M. J., Kavanagh, P. J., et al. 2024, *Science*, 383, 898
- [8] Greco, E., Miceli, M., Orlando, S., et al. 2021, *ApJ*, 908, L45
- [9] Greco, E., Miceli, M., Orlando, S., et al. 2022, *ApJ*, 931, 132
- [10] Grefenstette, B. W., Harrison, F. A., Boggs, S. E., et al. 2014, *Nature*, 506, 339
- [11] Holland-Ashford, T., Lopez, L. A., & Auchettl, K. 2020, *ApJ*, 889, 144
- [12] Hwang, U. & Laming, J. M. 2012, *ApJ*, 746, 130
- [13] Janka, H.-T. 2012, *Annual Review of Nuclear and Particle Science*, 62, 407
- [14] Janka, H.-T. 2017, “Neutrino-Driven Explosions” chapter in *Handbook of Supernovae* (edited by Athem W. Alsabti and Paul Murdin, ISBN 978-3-319-21845-8. Springer International Publishing, Switzerland), p. 1095
- [15] Jones, O. C., Kavanagh, P. J., Barlow, M. J., et al. 2023, *ApJ*, 958, 95

- [16] Laming, J. M. & Hwang, U. 2003, *ApJ*, 597, 347
- [17] Larsson, J., Fransson, C., Kjaer, K., et al. 2013, *ApJ*, 768, 89
- [18] Larsson, J., Fransson, C., Sargent, B., et al. 2023, *ApJ*, 949, L27
- [19] Larsson, J., Fransson, C., Spyromilio, J., et al. 2016, *ApJ*, 833, 147
- [20] Lee, J.-J., Park, S., Hughes, J. P., & Slane, P. O. 2014, *ApJ*, 789, 7
- [21] Matsuura, M., Boyer, M., Arendt, R. G., et al. 2024, *MNRAS*, 532, 3625
- [22] Milisavljevic, D. & Fesen, R. A. 2013, *ApJ*, 772, 134
- [23] Milisavljevic, D. & Fesen, R. A. 2015, *Science*, 347, 526
- [24] Milisavljevic, D., Temim, T., De Looze, I., et al. 2024, *ApJ*, 965, L27
- [25] Orlando, S., Greco, E., Hirai, R., et al. 2024, *ApJ*, 977, 118
- [26] Orlando, S., Janka, H.-T., Wongwathanarat, A., et al. 2025, *A&A*, 696, A188
- [27] Orlando, S., Janka, H.-T., Wongwathanarat, A., et al. 2025, *A&A*, 696, A108
- [28] Orlando, S., Miceli, M., Lo Cicero, U., & Ustamujic, S. 2023, in *Memorie della Societa Astronomica Italiana*, Vol. 94, 13
- [29] Orlando, S., Miceli, M., Ono, M., et al. 2025, *A&A*, 699, A305
- [30] Orlando, S., Miceli, M., Petruk, O., et al. 2019, *A&A*, 622, A73
- [31] Orlando, S., Miceli, M., Pumo, M. L., & Bocchino, F. 2015, *ApJ*, 810, 168
- [32] Orlando, S., Miceli, M., Pumo, M. L., & Bocchino, F. 2016, *ApJ*, 822, 22
- [33] Orlando, S., Ono, M., Nagataki, S., et al. 2020, *A&A*, 636, A22
- [34] Orlando, S., Pillitteri, I., Bocchino, F., Daricello, L., & Leonardi, L. 2019, *Research Notes of the American Astronomical Society*, 3, 176
- [35] Orlando, S., Wongwathanarat, A., Janka, H. T., et al. 2022, *A&A*, 666, A2
- [36] Orlando, S., Wongwathanarat, A., Janka, H. T., et al. 2021, *A&A*, 645, A66
- [37] Ravi, A. P., Park, S., Zhekov, S. A., et al. 2021, *ApJ*, 922, 140
- [38] Ravi, A. P., Park, S., Zhekov, S. A., et al. 2024, *ApJ*, 966, 147
- [39] Reed, J. E., Hester, J. J., Fabian, A. C., & Winkler, P. F. 1995, *ApJ*, 440, 706
- [40] Rho, J., Park, S.-H., Arendt, R., et al. 2024, *ApJ*, 969, L9
- [41] Sapienza, V., Miceli, M., Bamba, A., et al. 2024, *ApJ*, 961, L9

- [42] Sapienza, V., Miceli, M., Ono, M., et al. 2025, *ApJ*, 990, L5
- [43] Sun, L., Orlando, S., Greco, E., et al. 2025, *ApJ*, 981, 26
- [44] Thorstensen, J. R., Fesen, R. A., & van den Bergh, S. 2001, *AJ*, 122, 297
- [45] Vance, G. S., Young, P. A., Fryer, C. L., & Ellinger, C. I. 2020, *ApJ*, 895, 82
- [46] Weil, K. E., Fesen, R. A., Patnaude, D. J., et al. 2020, *ApJ*, 891, 116
- [47] Wongwathanarat, A., Janka, H. T., & Müller, E. 2013, *A&A*, 552, A126
- [48] Wongwathanarat, A., Janka, H.-T., Müller, E., Pllumbi, E., & Wanajo, S. 2017, *ApJ*, 842, 13
- [49] Wongwathanarat, A., Müller, E., & Janka, H.-T. 2015, *A&A*, 577, A48
- [50] Xrism Collaboration, Audard, M., Awaki, H., et al. 2025, *PASJ*, 77, S193